World Academy of Science, Engineering and Technology
International Journal of Materials and Metallurgical Engineering
Vol:9, No:1, 2015

Structural and Optical Properties of Pr^{3+} Doped ZnO and PVA:$Zn_{98}Pr_2O$ Nanocomposite Free Standing Film

Pandiyarajan Thangaraj, Mangalaraja Ramalinga Viswanathan, Karthikeyan Balasubramanian, Héctor D. Mansilla, José Ruiz, David Contreras

***Abstract*—**In this work, we report, a systematic study on the structural and optical properties of Pr-doped ZnO nanostructures and PVA:$Zn_{98}Pr_2O$ polymer matrix nanocomposites free standing films. These particles are synthesized through simple wet chemical route and solution casting technique at room temperature, respectively. Structural studies carried out by X-ray diffraction method confirm that the prepared pure ZnO and Pr doped ZnO nanostructures are in hexagonal wurtzite structure and the microstrain is increased upon doping. TEM analysis reveals that the prepared materials are in sheet like nature. Absorption spectra show free excitonic absorption band at 370 nm and red shift for the Pr doped ZnO nanostructures. The PVA:$Zn_{98}Pr_2O$ composite film exhibits both free excitonic and PVA absorption bands at 282 nm. Fourier transform infrared spectral studies confirm the presence of A_1 (TO) and E_1 (TO) modes of Zn-O bond vibration and the formation of polymer composite materials.

***Keywords*—**Pr doped ZnO, polymer nanocomposites, optical properties.

I. Introduction

SEMICONDUCTOR nanostructured materials have enhanced mechanical, optical, electrical and thermal properties that are quite different from the bulk [1]-[3]. Among them, oxide semiconductor nanostructures are gained much attention because of versatile properties and their application in various fields. Especially, ZnO is an II-VI wide band gap semiconductor with band gap of 3.37 eV and very high exciton binding energy of 60 meV at room temperature compared to the other materials in this family [4]. ZnO has wide range of technological application in various fields like opto-electronic fields [5], photocatalysis [6], sensors [7], and antimicrobial agents [8]. There are several techniques like sol–gel [9], hydrothermal [10], laser ablation [11], and wet chemical [12] developed for the synthesis of ZnO nanostructures. Among these, wet chemical method is the simplest technique to prepare ZnO nanostructures at room temperatures and has the ability to control the morphology and size.

Doping of foreign trace element into semiconductors is a promising method that is efficient, cost effective, and easy to manipulate their optical and electrical properties. It is known that the optical and electrical properties of the rare earth (RE) ions depend on the host matrix and dopant compositions. Trivalent rare earth doped semiconductors are technologically important materials in optoelectronic devices like visible light emitting phosphors for displays. Among trivalent ions, Pr^{3+} ion has unique optical properties along with tunable emissions from the blue region to the near infrared regime. There are reports available on the structural and optical properties of Pr^{3+} doped ZnO nanostructures. For instance, Ilanchezhiyan and co-workers have studied the effect of Pr doping on structural and optical properties of ZnO nanostructures [13]. Inoue et al. have observed the enhancement in the green photoluminescence from ZnO:Pr powders [14]. Li et al. have studied the optical properties with respect to the effects of aging and Pr doping on ZnO quantum dots [15]. Ohashi and his group have reported the nonlinear current-voltage characteristics of Pr doped ZnO ceramics [16]. Similarly, Mass transport properties of Pr-based ZnO varistors have been studied by Chun et al. [17].

Optical properties of semiconducting materials can also be tuned/controlled by tailoring its size, shape and surface capping. Incorporation of nanomaterials into polymers makes new kind of materials which have enhanced physical properties and show potential applications in various fields like flexible light emitting diodes [18] sensors [19] and optical power limiters [20]. Among the polymers, poly vinyl alcohol (PVA), an eco-friendly, water soluble and easily film forming material at room temperature, exhibits an excellent host matrix. Dispersion of ZnO nanostructures into PVA shows enhanced optical properties.

Owing importance to the aforementioned aspects, we have carried out a systematic study of Pr-doped ZnO nanostructures and PVA:$Zn_{98}Pr_2O$ polymer nanocomposites free standing films, synthesized through wet chemical route and solution casting techniques at room temperature, respectively. The influence of Pr ion and PVA capping on the structural, morphology and optical properties of the ZnO nanostructures are also studied in detail.

II. Experimental

All chemicals used in the experiment were of high purity reagents purchased from Sigma-Aldrich. ZnO is prepared by adding drop-wise 100 ml of 0.1M NaOH dissolved in double

Pandiyarajan.T and Mangalaraja R. V. are with the Advanced Ceramics and Nanotechnology Laboratory, Department of Materials Engineering, University of Concepcion, Concepcion, Chile (e-mail: rtpandiyarajan@gmail.com, mangal@udec.cl).

Karthikeyan. B. is with the Department of Physics, National Institute of Technology, Tiruchirappalli 620 015, India.

H.D.Mansilla is with the Departament of Organic Chemistry, Faculty of Chemical Sciences, Universidad de Concepcion, Concepcion, Chile

José Ruiz is with the Renewable Resources Laboratory, Biotechnology Center, Universidad de Concepción, Concepción, Chile

D. Contreras is with the Department of Analytical and Inorganic Chemistry, Faculty of Chemical Sciences, Center for Biotechnology, University of Concepcion, Concepcion, Chile

distilled water into 100 ml of 0.05 M zinc nitrate hexahydrate ($Zn(NO_3)_2$•$6H_2O$) dissolved in double distilled water. The formed white gel was kept at room temperature for 12 hours to get precipitated. Similarly, Pr doped ZnO samples were prepared by mixing 0.002 M solution of praseodymium nitrate hexahydrate (Pr $(NO_3)_3$•$6H_2O$) with 0.048M zinc nitrate solution. Then 0.1M NaOH solution was added drop-wise into the above mixture, a white coloured gel was obtained and kept at room temperature for over 12 hours. The precipitates were collected and dried in a hot air oven at 60°C for four hours. On the other hand, PVA:$Zn_{98}Pr_2O$ free standing film were prepared by the following procedure: Initially, 1.0 g of PVA (M.Wt. 19,000; 98% solubility) was dissolved into 20 ml of hot distilled water and stirred for about a half an hour to form the clear solution. 5 mg of prepared $Zn_{98}Pr_2O$ nanostructures was dispersed into the 3 ml of double distilled water separately. The prepared $Zn_{98}Pr_2O$ solution was added into the PVA solutions and stirred for half an hour to get uniform dispersion. Then the solution was poured in the petridish and kept at room temperature over 10 days of period. The obtained films are transparent with free standing in nature which is shown in inset of Fig. 5. The samples are code denoted as ZnO, $Zn_{98}Pr_2O$ and PVA:$Zn_{98}Pr_2O$, respectively.

The crystal structure of the pure ZnO, Pr doped ZnO nanostructures and PVA:$Zn_{98}Pr_2O$ composite film formations were investigated by the X-ray diffraction (XRD) technique (Bruker, D4 Endeavor). The power of the XRD (Cu–Kα radiation) was fixed at 40 kV and 20 mA. The measurements were made with XRD diffracion angle (2θ) in the range 10–80°. Morphology of the prepared nanostructures was carried out by transmission electron microscope (TEM, JEOL JEM 2000 EX). To study, optical characterization, 1 mg of pure ZnO and Pr doped ZnO nanostructured samples were dispersed in 15 ml doubly distilled water and then sonicated for about 30 minutes. Absorption and transmission measurements were carried out using a Shimadzu spectrophotometer. Fourier transform infrared spectroscopy (FTIR) absorption measurements were carried out using Perkin Elmer spectrometer by KBr pellet technique in the range 4000–350 cm^{-1}.

III. Results and Discussion

A. Structural Studies

X-ray diffraction pattern of the synthesized ZnO, $Zn_{98}Pr_2O$ nanostructures and PVA:$Zn_{98}Pr_2O$ nanocomposite film is shown in Fig. 1. ZnO nanostructures show strong and sharp peaks which are well assigned to the wurtzite structure. The peaks are located at the angles (2θ) of 31.71°, 34.35° and 36.18°, which corresponds to (100), (002) and (101) planes of the ZnO, similarly the other peaks are found in the 2θ angles of 47.45°, 56.51°, 62.76°, 66.25°, 67.85° and 68.99° corresponds to (102), (110) (103), (200), (112) and (201) planes of the ZnO which confirms wurtzite structure, respectively. The PVA film shows broad peaks around the 2θ angles of 19.45° and 41.05° corresponds to the crystalline PVA (JCPDS: 53-1487). Similarly, for PVA:$Zn_{98}Pr_2O$ composite films exhibit both diffraction peaks of PVA and ZnO structures. Enlarged view of XRD pattern of polymer nanocomposite film in the range of 20° to 45° is shown in the inset of Fig. 1 and it is clearly shows the appearance of ZnO peaks which conclude the formation of the composite materials.

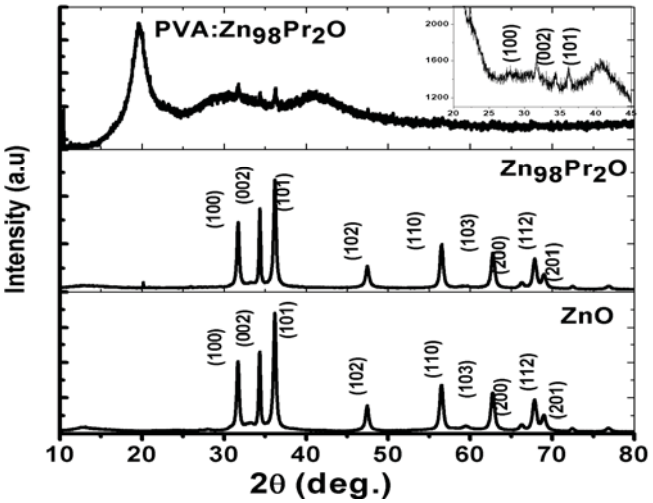

Fig. 1 XRD spectra of pure ZnO, Pr doped ZnO nanostructures and PVA:$Zn_{98}Pr_2O$ polymer nanocomposite free standing film

B. Microstrain Analysis

X-ray profile analysis is a simple and powerful technique to quantify the crystallite size and lattice strain. Williamson-Hall had proposed the diffraction line broadening is due to crystallite size and strain contribution as a function of diffraction angle and can be written in the form of a mathematical expression $\beta_{hkl} = \beta_t + \beta_\varepsilon$ [21] where, β_t is due to crystallite size contribution, β_ε is due to strain induced broadening and β_{hkl} is the width of the half maximum intensity of diffracted peak. The diffraction peaks were fitted using Pearson VII function to calculate full width at half maximum (FWHM). Crystallite size (*t*) contribution can be calculated by using Scherer formula $\beta_t = \frac{k\lambda}{t\cos\theta}$, where, *k* is the shape factor, λ is the wavelength of the X-ray used (1.54056×10^{-10} m) and β_t is FWHM of the diffracted peak. Similarly, strain contribution can be calculated by $\beta_\varepsilon = 4\varepsilon\tan\theta$, where '$\varepsilon$' is the microstrain. It is clear that the line broadening is a combination of crystallite size and strain and it is represented by $\beta_{hkl} = \left(\frac{K\lambda}{t\cos\theta}\right) + (4\varepsilon\tan\theta)$. This can be further simplified as $\beta_{hkl}\cos\theta_{hkl} = \left(\frac{K\lambda}{t}\right) + (4\varepsilon\sin\theta_{hkl})$. The value of $\beta_{hkl}\cos\theta_{hkl}$ as a function of $4\sin\theta_{hkl}$ is plotted and is shown in Fig. 2. The microstrain can be obtained by measuring the slope of the linear fit of data and the calculated microstrain values are 0.00248±0.000628 and 0.00252±0.000846 for ZnO and $Zn_{98}Pr_2O$, respectively. It is

clear that the doping of Pr^{3+} into ZnO matrix leads to increase in microstrain value of the system. Microstrain calculations are not performed for the polymer nanocomposite film due to decrease in peak intensity of ZnO into the polymer matrix.

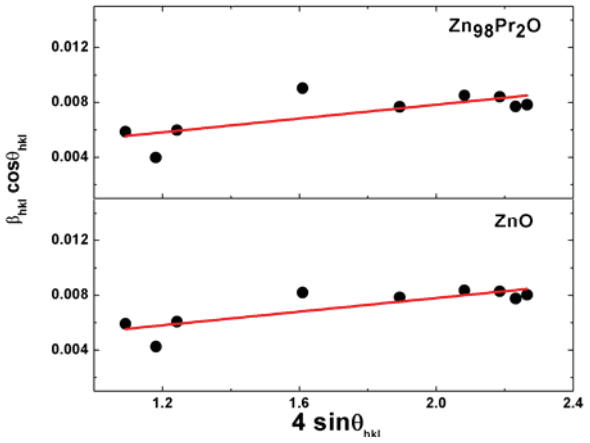

Fig. 2 Williamson-Hall analysis of pure ZnO and Pr doped ZnO nanostructures

C. Morphological Studies

Morphology of the synthesized materials was analyzed through transmission electron microscopy (TEM) and is shown in Figs. 3 (a)-(c).

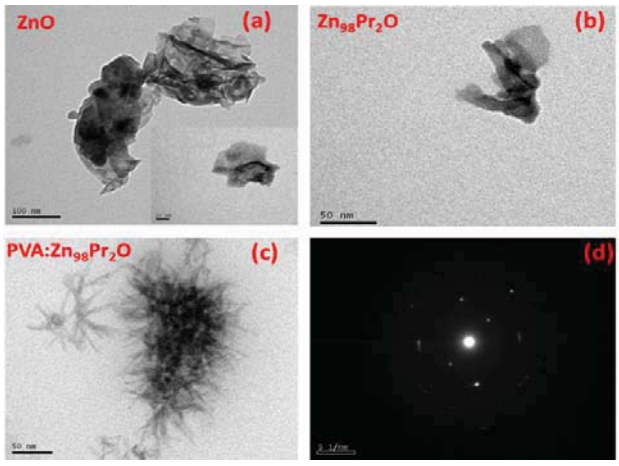

Fig. 3 (a) TEM images of pure ZnO (b) Pr doped ZnO nanostructures (c) PVA:$Zn_{98}Pr_2O$ polymer nanocomposite free standing film and (d) Selected area diffraction pattern of Pr doped ZnO nanostructure.

Images reveal that the ZnO and $Zn_{98}Pr_2O$ are in sheet like structure. PVA:$Zn_{98}Pr_2O$ composite shows brush like nature because of the polymer backbone. Fig. 3 (d) represents selected area diffraction pattern of Pr doped ZnO nanostructures in which the well-defined dots confirm the crystalline nature of the materials.

D. Optical Properties

Optical absorption spectra of the pure ZnO and Pr doped ZnO dispersed in distilled water are shown in Fig. 4. Spectra show a strong absorption band at 370 nm is due to the free excitonic absorption of ZnO nanostructures. A significant red shift (373 nm) in the absorption band was observed in Pr doped ZnO nanostructures and is due to the formation of electronic state impurity band into the band gap of ZnO by Pr (4f) electronic localized states. The merging of electronic state with the bottom of the conduction band could be reasoned for the reduction in the band gap. The PVA:$Zn_{98}Pr_2O$ polymer film shows absorption bands at ~ 282 nm and 368 nm and these arise due to the presence of carbonyl containing structures connected to the PVA polymeric chains, mainly at the ends [22] and free excitonic absorption of ZnO nanostructures, respectively.

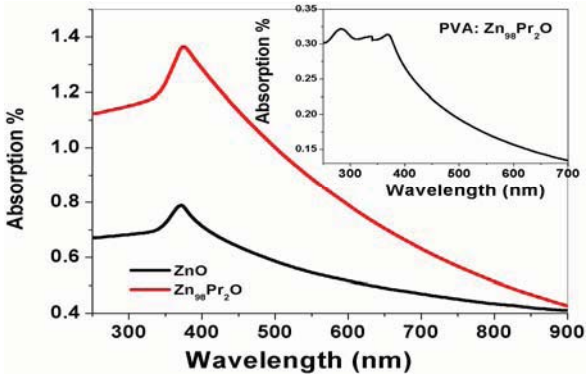

Fig. 4 UV-visible spectra of pure ZnO and Pr doped ZnO nanostructures. Inset represents for the PVA:$Zn_{98}Pr_2O$ polymer nanocomposite free standing film

The presence of ZnO band confirms the ZnO nanostructures are embedded into the PVA matrix. In general, the absorption transitions of Pr^{3+} ions occurs at 445, 470, 485 and 593 nm which are attributed to the $^3H_4$-$^3P_2$, $^3H_4$-$^3P_1$, $^3H_4$-$^3P_0$ and $^3H_4$-D_2 transitions, respectively [23]. In the present system there were no transitions observed.

Fig. 5 depicts the transmission spectrum of as prepared film. It was observed that 60 to 78 % of transparency in the visible and near IR region. The as prepared PVA:$Zn_{98}Pr_2O$ polymer nanocomposite free standing film is shown in the inset of Fig. 5.

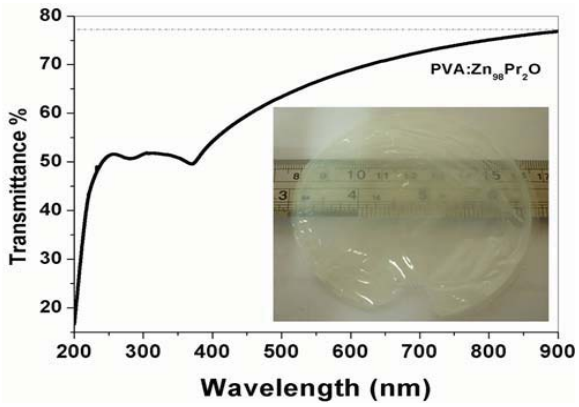

Fig. 5 Transmission spectrum of PVA:$Zn_{98}Pr_2O$ polymer nanocomposite free standing film. Inset shows the as prepared the PVA: $Zn_{98}Pr_2O$ polymer nanocomposite free standing film

E. Vibrational Studies

FTIR spectra of pure ZnO, Pr doped ZnO and PVA:$Zn_{98}Pr_2O$ polymer nanocomposite free standing film are displayed in Fig. 6 (a). The strong transmission bands appear at 3380 cm^{-1} and 1555 cm^{-1} are due to the stretching and bending modes of hydroxyl (O–H) group of H_2O, respectively [24]. These bands are due to the moisture adsorbed by KBr pellets while performing FTIR experiment in ambient environment.

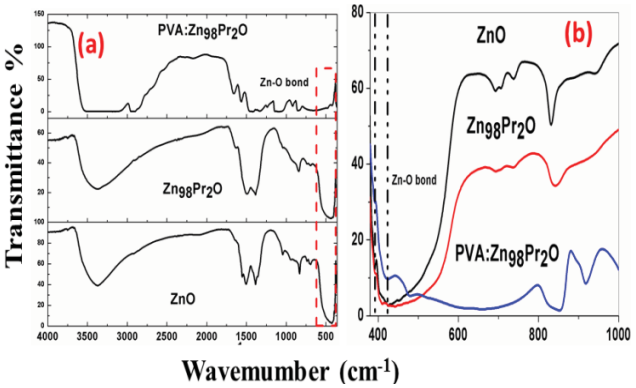

Fig. 6 (a) FTIR spectra of pure ZnO, Pr doped ZnO nanostructures and PVA:$Zn_{98}Pr_2O$ polymer nanocomposite free standing film (b) Expanded view of FTIR spectra in the range between 350 to 100 cm^{-1}

Usually, metal-oxygen bands are appeared in the range between 350 cm^{-1} to 700 cm^{-1}. In order to identify precisely such modes, the FTIR spectra were recorded in the region of 350 cm^{-1} to 4000 cm^{-1}. The bands observed at 392 cm^{-1} and 424 cm^{-1} are due to the stretching modes of Zn-O bond [25], which corresponds the signature of stretching polar vibrational modes of A_1 (TO) and E_1 (TO), respectively. The band appears in the higher wavenumber side could be assigned to the organic compounds. The band appears at 1379 cm^{-1} could be assigned to the vibrations of the N-O bond [26] which comes from the nitrate compound present in the precursors. In addition to these bands, polymer composite film exhibits additional bands which are related to the PVA molecules. The vibrational band at 2932 cm^{-1} refers to the stretching of C-H from PVA chains and the peaks at 1100 cm^{-1} is assigned to the C-O-C vibrations [27]. The appearance of Zn-O bond vibrations and polymer molecules confirms the formation of composite materials.

IV. Conclusion

In summary, an investigation on the structural and optical properties of Pr doped ZnO nanostructures and PVA:$Zn_{98}Pr_2O$ polymer nanocomposite free standing film was studied. Crystalline nature of the particles and formation of composite structure were analyzed by XRD measurements. Sheet and brush like morphological structures for Pr doped ZnO and PVA:$Zn_{98}Pr_2O$, respectively, were observed by TEM analysis. Optical absorption spectra revealed that there was a red shift in the excitonic absorption band upon doping. FTIR spectra confirmed the presence of Zn-O bond and composite formation. Furthermore, a detailed steady state and time resolved photoluminescence measurement of Pr doped ZnO nanostructures and PVA:$Zn_{98}Pr_2O$ are needed to identify the emission properties of polymer films.

Acknowledgment

The authors gratefully acknowledge the FONDECYT Post-doctoral Project No.: 3140178 and FONDECYT No.: 1130916, Government of Chile, Santiago, for the financial assistance.

References

[1] L. Irimpan, V. P. N. Nampoori, P. Radhakrishnan, A. Deepthy, and Bindu Krishnan, "Size dependent fluorescence spectroscopy of nanocolloids of ZnO," *J. Appl. Phys.,* vol. 102, pp. 063524-6, September 2007.

[2] Nikolaos Tombros, Alina Veligura, Juliane Junesch, Marcos H. D. Guimarães, Ivan J. Vera-Marun, Harry T. Jonkma, Bart J. van Wees, "Quantized conductance of a suspended graphene nanoconstriction," *Nature Physics* vol. 7, pp. 697–700, June 2011.

[3] R. Viswanatha, S. Sapra, B. Satpati, P. V. Satyam, B. N. Dev and D. D. Sarma, "Understanding the quantum size effects in ZnO nanocrystals," *J. Mater. Chem.,* vol. 14, pp. 661-668, October 2004.

[4] M. Dvorak, S.H. Wei and Z. Wu, "Origin of the Variation of Exciton Binding Energy in Semiconductors," *Phys. Rev. Lett.,* vol. 110, pp. 016402 (1-4), January 2013.

[5] A. E. Suliman, Y. Tang and L. Xu, "Preparation of ZnO nanostructures and nanosheets and their application to dye-sensitized solar cells," *Solar Energy Materials and Solar Cells* vol. 91, pp. 1658–1662, November 2007.

[6] P. Li , Z. Wei , T. Wu, Q. Peng and Y.Li, "Au–ZnO Hybrid Nanopyramids and Their Photocatalytic Properties" *J. Am. Chem. Soc.,* vol. 133, pp 5660–5663, March 2011.

[7] Z. Fan, D. Wang, P. C. Chang, W.Y. Tseng and J. G. Lu, "ZnO nanowire field-effect transistor and oxygen sensing property," *Appl. Phys. Lett.*, vol. 85, pp. 5923-5925, December 2004.

[8] S. Nair, A. Sasidharan, V. V. Divya Rani, D. Menon, S. Nair, K. Manzoor and S. Raina, "Role of size scale of ZnO nanostructures and microparticles on toxicity toward bacteria and osteoblast cancer cells," *J Mater Sci: Mater Med.,* vol.20, pp. S235–S241, April 2009.

[9] K.F. Lin, H. M. Cheng, H.C. Hsu, L.J. Lin, and W.F. Hsieh, "Band gap variation of size-controlled ZnO quantum dots synthesized by sol–gel method," *Chem. Phys. Lett.,* vol. 409, pp. 208–211, June 2005.

[10] H. Zhang, D. Yang, Y. Ji, X. Ma, J. Xu, and D. Que, "Low Temperature Synthesis of Flowerlike ZnO Nanostructures by Cetyltrimethylammonium Bromide-Assisted Hydrothermal Process", *J. Phys. Chem. B*, vol. 108, pp 3955–3958, March 2004.

[11] A.B. Hartanto, X. Ning, Y. Nakata, and T. Okada, "Growth mechanism of ZnO nanorods from nanoparticles formed in a laser ablation plume", *Appl. Phys. A* vol. 78, pp. 299–301, February 2004.

[12] J. Wang and L. Gao, "Wet chemical synthesis of ultralong and straight single-crystalline ZnO nanowires and their excellent UV emission properties," *J. Mater. Chem.,* vol. 13, pp. 2551-2554, August 2003.

[13] P. Ilanchezhiyan, G. Mohan Kumar, M. Subramanian and R. Jayavel, "Effect of Pr doping on the structural and optical properties of ZnO nanorods," Mater. Sci. Eng. B vol. 175, pp. 238–242 December 2010.

[14] Y. Inoue, M. Okamoto and J. Morimoto, "Enhancement of green photoluminescence from ZnO:Pr powders," *J. Mater. Res.,* vol. 21, pp. 1476-1483 June 2006.

[15] H. Li, K. Luo, M. Xia and P. W. Wang, "Synthesis and optical properties of Pr^{3+}-doped ZnO quantum dots" *J. Non-Crystalline Solids,* vol. 383, pp.176–180 January 2014.

[16] N. Ohashi, S. Mitarai and O. Fukunaga, "Magnetization and Electric Properties of Pr-doped ZnO," *J. Electroceram.,* Vol 4, pp. 61–68 December 1999.

[17] S.Y. Chun and N. Mizutani, "Mass transport via grain boundary in Pr-based ZnO varistors and related electrical effects," *Mater. Sci. Eng. B* vol. 79, pp. 1–5 January 2001.

[18] G. H. Gelinck, H. E. A. Huitema, E. Veenendaal, E. Cantatore, L. Schrijnemakers, J. B. P. H. van der Putten, T. C. T. Geuns, M. Beenhakkers, J. B. Giesbers, B. H. Huisman, E. J. Meijer, E. M. Benito,

F. J. Touwslager, A. W. Marsman, B.J. E. van Rens and D. M. D. Leeuw, "Flexible active-matrix displays and shift registers based on solution-processed organic transistors," *Nature Mater.,* vol. 3, pp.106-110, January 2004.

[19] M. Cavallini, J. G. Segura, D. R. Molina, M. Massi, C. Albonetti, C. Rovira, J. Veciana and F. Biscarini, "Magnetic Information Storage on Polymers by Using Patterned Single-Molecule Magnets," *Angew. Chem. Int. Ed.,* vol. 44, pp. 888-892 January 2005.

[20] B. Karthikeyan, M. Anija, Reji Philip, In situ synthesis and nonlinear optical properties of Au:Ag nanocomposite polymer films, *Appl. Phys. Lett.,* vol. 88, pp. 053104-3 January 2006.

[21] Y. Rosenberg, V.S. Machavariani, V. Voronel, S. Garber, A. Rubshtein, A.I. Frenkel, E.A. Stern, "Strain energy density in the X-ray powder diffraction from mixed crystals and alloys," *J. Phys., Condens Matter.,* vol. 12, pp. 8081–8088, July 2000.

[22] S. Clemenson, L. David, and E. Espuche, "Structure and morphology of nanocomposite films prepared from polyvinyl alcohol and silver nitrate: Influence of thermal treatmen," *J. Polymer Sci.: Part A: Polymer Chem.,* vol. 45, pp 2657–2672, July 2007.

[23] H. Li, K. Luo, M. Xia, P. W. Wang, "Synthesis and optical properties of Pr^{3+} doped ZnO quantum dots", J. Non-Crystalline Solids vol. 383, pp. 176–180, June 2014.

[24] K. Nakamoto, *Infrared Spectra of Inorganic and Coordination Compounds*, Wiley, New York, 1973.

[25] M. Ghosh, N. Dilawar, A.K. Bandyopadhyay, A.K. Raychaudhuri, "Phonon dynamics of Zn (Mg, Cd) O alloy nanostructures and their phase segregation," *J. Appl. Phys.,* vol. 106, pp. 084306 (1-6) October 2009.

[26] T. Pandiyarajan, B. Karthikeyan, "Optical properties of annealing induced post growth ZnO:$ZnFe_2O_4$ nanocomposites," *Spectrochimica Acta A*, vol. 106, pp. 247–252, January 2013.

[27] H. S. Mansur, C. M. Sadahira, A. N. Souza, A.A.P. Mansur, "FTIR spectroscopy characterization of poly (vinyl alcohol) hydrogel with different hydrolysis degree and chemically crosslinked with glutaraldehyde," *Mater. Sci. Eng. C* vol. 28, pp. 539–548, December 2008.